ISRAA UNIVERSITY JOURNAL OF APPLIED SCIENCES
ISSN : 2523-0522
Volume 2 : issue 1 , October , 2018

Estimation of Temperature in Aluminum Plasma Using Laser Induced Breakdown Spectroscopy

Shawqi A. M. Mansour [*3]

Received Jan 2018; accepted April 2018

Abstract: *Plasma produced by a 1.064 µm pulsed with a pulse duration of 6ns focused onto a pure aluminum solid sample (~99.99%) in air at atmospheric pressure is studied spectroscopy. An Echelle spectrograph coupled with a gate intensified charge coupled detector is used to record the plasma emissions. The plasma temperature was measured by time-resolved spectroscopy of aluminum neutral atom line emissions in the time window of 1-5 µs, using Saha-Boltzmann plot method. The aluminum neutral lines were found to suffer from optical thickness over the entire delay times. Analytical relations were used and experimental procedures devised for evaluation of the self-absorption coefficients of several Al-lines, which are important to get reliable temperature measurements. The results shows that Al (I) lines have highest plasma temperature of 1.427 eV before correction against self absorption, while revealed a lowest temperature of 1.092 eV after correction.*

Key words: *Optical emission spectroscopy (OES), Electron temperature, Self-bsorption effect (SA),* $H_\alpha - line(656.27\ nm)$, *LIBS.*

[3] Shawqi A. M. Mansour, Energy and Sustainable Environment Center, Palestine Technical College – Deir El Balah, Engineering Department-Deir El - Balah , Palestine. dr_shmansour@yahoo.com.

1. INTRODUCTION

Laser-induced breakdown spectroscopy is a powerful analytical technique with a wide range of applications concerning both fundamental purposes and material analysis **(Tognoni et al. 2002)** , **(Aragón et al. 2005)**, **(Bengoechea et al. 2006)**, **(Colón and Alonso-Medina 2006)**. LIBS techniques is unique in that it may be used to chemically analyze rocks, glasses, metals, sand, teeth, bones, powders, hazardous materials, liquids, plant, biological material, polymers, ceramics, etc. **(Thoron, 1988)**, **(Amoruso et al., 1997)**. Aluminum metal as an abrasive material due to its hardness and as refractory material due to its high melting point remained a subject of interest for many researchers. **(Lu et al., 1999)** studied the aluminum plasma generated by an excimer (248nm) in vacuum using an optical multichannel analyzer. **(Colón et al., 1993)** measured the Stark broadening parameters of some of the All transition lines in the nitrogen atmosphere. **(Body and Shadwich , 2001)** presented new instrumentation variation on LIBS and used it for the analysis of coal by detecting AL, Si, Mg, Ca, Fe, Na, C, K and H as its key organic components. The consequence of the ambient gas pressure on the spectral intensity of the zinc-aluminum alloy was studied by **(Kim et al., 1997)** using a Nd: YAG laser at 1064 nm and reported that the spectral intensity of the neutral aluminum line at 309.27 nm increases with the ambient pressure in air and argon. **(Handoco et al., 2006)** reported the time-resolved emission spectroscopic investigations of pulse laser-ablated plasma of ZrO_2 and Al_2O_3.

In this paper, we shall adopt a straightforward procedure to calculate the self-absorption coefficients of the plasma to the resonance lines at 308.21nm, 309..27nm, 394.40nm, and 396.15nm of neutral aluminum via comparison of the electron densities evaluated using the Stark broadening of the aluminum lines to the electron density as deduced from the optically thin $H_\alpha - line$ **(Mansour, 2015)**. The induced plasma temperature was determined after the correction of aluminum intensities lines against self-absorption effect.

1. DETERMINATION OF THE ELECTRON TEMPERATURE

Knowledge of the plasma temperature is vital to understand the dissociation, atomization, ionization and excitation processes occurring in the plasma and helpful in utilizing the plasma to maximize analytical potential of LIBS **(McWhirter R. W. P., 1965)**. The temperature, T defined as the particular form of energy and it can determine the equilibrium distribution of energy among the different state of the particle assembled. It may happen that the equilibrium distributions exist for one form of energy but not for another. Thermodynamic equilibrium will exist when all form of energy distribution is described by the same temperature.

In the case of Local Thermodynamic Equilibrium (LTE), the excitation temperature, $T_{exc.}$ is equal to temperature of electron, T_e and T_i temperature of heavy particle i.e., atom and ions, $T_{exc.} = T_e = T_i$ where, T_i is the temperature describing the photon distribution. The escape of photon is associated with spatial gradient in the plasma and to time-dependent regimes, so that LTE can be established **(Fujimoto, 2004)**, **(Van Der Mullen, 1990)**, and **(Capitelli et al., 2000)**.

In LIBS plasma the ionization degree is sufficiently high, this completion dominated by the electron, i.e. $T_{exc.} \sim T_i$ and just a small perturbation that is usually be neglected can be expected from the temperatures of electron and heavy particle **(Cristoforetti et al., 2010)**. In typical LIBS plasma only, neutral atom and singly charged ion are presents to a significant degree. Therefore, only neutral and singly ionized particle will be considered. Under LTE condition, the population of the excited level for each species follows a Boltzmann distribution **(Miziolek et al., 2006**). The condition of atomic and ionic state should be populated mainly by electron collision other than radiation, to ensure it has high collision rate the electron density must be sufficient. The minimum limit for electron density n_e is,

$$\boldsymbol{n_e = 1.6 \times 10^{12} T^{1/2} (\Delta E)^3} \ldots\ldots\ldots\ldots\ldots\ldots\ldots\ldots (\mathbf{1})$$

where ΔE is the highest energy to hold the LTE condition, and T is the plasma temperature. This limit is given by McWhirter criterion to fulfill during the first stage of plasma lifetime. This criterion is necessary even though it insufficient for the condition **(Miziolek et al., 2006)**. The excitation temperature control the population of atomic and ionic energy level must be same as the ionization temperature. It resolved the distribution of atom of the same element in the different ionization stages. It describe in Saha equation where the neutral and singly ionized species of the same element can be written as,

$$\boldsymbol{n_e \frac{n^{II}}{n^I} = \frac{2(2\pi m_e kT)^{\frac{3}{2}}}{h^3} \frac{2U^{II}(T)}{U^I(T)} e^{-\frac{E_{ion}}{kT}}} \ldots\ldots\ldots\ldots (\mathbf{2})$$

Where, n_e is the plasma electron density, n^I and n^{II} are the number densities of the neutral atomic species and the single ionized species, respectively, Eion is the ionization potential of the neutral species in its ground state, me is the electron mass, and h is Planck's constant. In accurate calculations, the ionization potential lowering factor E_{ion} should be taken into accounts for the typical value being on the order of 0.1 eV. In the measurement of plasma temperature, many methods have described it based on the absolute or relative line intensity (line pair ratio or Boltzmann plot), the ratio line to the continuum intensity. The method was depending on the

experimental condition whether it is suitable or not **(Bye and Scheeline, 2003)**. Boltzmann equation is use to relate the population of an excited level to the total number density of the species in the plasma. After the linearization, the formula of Boltzmann plot obtained was:

$$ln\frac{I_{ij}}{g_i\ A_{ij}} = ln\left(\frac{n^S(T)}{U^S(T)}\right) - \frac{E_i}{kT} \ldots\ldots\ldots\ldots\ldots\ldots\ldots (3)$$

The left hand side of the equation (3) versus E_i was plotted and has a slope of -1/kT. The plasma temperature can be calculated without ns and $U^s(T)$. The gradient usually gives negative slope. The electron can be derived from the intensity ratio of the two lines corresponding to the different ionization stages of the same element when the plasma is near to LTE condition. The formula of Saha equation refer to the ratio of the total number densities of two ionization stages of the same element. Most of the research is using Stark broadening method and use the line intensity ratio to determine the electron density of plasma **(Detalle et al., 2001)**, **(Le Drogoff et al., 2010)**, (**Lee et al., 1992)** and **(Sabsabi et al., 1995)**.

2. DETERMINATION OF THE ELECTRON DENSITY

The electron density is an important parameter used to describe the plasma environment and it is crucial for establishing its equilibrium status. It can be evaluated from the profile of the spectral line emitted through a line of sight of laser-produced plasma, which is the result of several spectral broadening and shift mechanisms **(Griem, 1964**) and **(Konjevic et al., 2000)**. In the experimental conditions of the present work, the main contribution to line widths arises from Stark effect where the contributions of other mechanisms of broadening can be neglected. The FWHM of the spectral line under study $\Delta\lambda_{1l2}$ was determined by a Voigt fitting procedure. Hence, the electron density (in cm^{-3}) can be determined from the line width as.

$$\Delta\lambda_{1/2} \cong 2\omega\left(\frac{n_e}{N}\right) \ldots\ldots\ldots\ldots\ldots\ldots\ldots\ldots\ldots\ldots\ldots\ldots\ldots (4)$$

where, ω is the electron impact width parameter, Nr is the reference electron density which equal to $(10^{16}cm^{-3})$ for neutral atoms and $(10^{17}cm^{-3})$ for singly charged ions **(Konjevic, 2000)** and **(Konjevic et al. , 2003)**. In the special case of the hydrogen $n_e\ (H_\alpha) - line$ the electron density can be related to the Lorentzian half width at the half of the maximum $\Delta\lambda_{1l2}$ through the relation **(Griem, 1964)**,

$$H_\alpha = 8.02 \times 10^{12}\left(\frac{\Delta\lambda_S}{\alpha_{1/2}}\right)cm^{-3} \ldots\ldots\ldots\ldots\ldots\ldots (5)$$

Where, $\Delta\lambda_s$ is the intrinsic full width at half of maximum (FWHM) of the spectral line in Angstrom, and $\alpha_{1/2}$ is the half width of the reduced Stark profiles in Angstrom. Precise values of α_{1l2} for the Balmer series can be found in **(Konjevic et al., 2003)**, **(Kepple and Griem, 1968)** and

(Almen, 1987). However, when the laser beam is focused on the target, the ablation of the target takes place, and due to the density gradient, the plasma rapidly expands.

3. SELF-ABSORPTİON ANALYSİS:

The self-absorption (SA) coefficient focused on line (λ_o) results from the expression is **(Griem, 1974)**,

$$S.A = \frac{I(\lambda_o)}{I_o(\lambda_o)} = \frac{[1 - e^{-k(\lambda_o)l}]}{[K(\lambda_0)l]} \dots\dots\dots\dots\dots\dots\dots (6)$$

where, $I(\lambda_o)$is the relative intensity subject to self-absorption, $I_o(\lambda_o)$ is the same as the former, but without self-absorption, and $k(\lambda_o)l = \tau(\lambda_o)$ is the plasma optical path until the center of the line. On the other hand, the self-absorption coefficients of Al I- lines have been estimated from the basic relation as described in **(El Sherbini et al., 2005)**, **(Mansour, 2015)**, **(Mansour et al., 2015)**, and **(Mansour, (2017)**.

$$S.A = \left(\frac{\Delta\lambda}{\Delta\lambda_o}\right)^{1/\alpha} = \left(\frac{n_e\ (line)}{n_e(H_\alpha)}\right)^{1/\alpha} \dots\dots\dots\dots\dots\dots\dots (7)$$

Where, n_e(line) is the electron density of the line which suffering from self-absorption effect, $n_e\ (H_\alpha)$ is the electron density of $H_\alpha - line$ free from self-absorption and $\alpha = 0.56$. Hence, the researchers utilized Eq. (3) in order to calculate the amount of absorption (SA).

4. Experimental details

Figure 1 show the schematic diagram of LIBS experiment. The Q-Switched Nd:YAG laser (Quintal, model Brilliant B) was operated at fundamental wavelength of 1064 nm, the repetition rate of 10 Hz and pulse width of 6 ns, which capable of delivering 670 mJ at 1064 nm. An absolute calibrated power-meter (Ophier, model 1z02165) was used for measuring a fraction of the laser light reflected from a quartz beam splitter to monitor the incident laser energy. The laser beam was focused on the target using convex lens of focal length 10cm. The sample was mounted on a three dimensional sample stage, which was rotated to avoid the non-uniform pitting of the target. The distance between the focusing lens and the sample was kept at 9.5cm, less than the focal length of the lens to prevent any breakdown of the ambient air in the front of the target. The spectra were obtained by averaging three single data of shots under identical experimental conditions. The laser spot was measured at the target surface and gives a circle of diameter of 2mm because of the deflagration effect and hence the laser energy per pulse of the order of 327.42mJ was measured at the target surface. The radiations emitted by the plasma were collected by quarts optical fiber (with

a 25µm diameter) placed at right angle to the direction of the laser beam. The optical fiber was connected with detection system consists of Echelle spectrograph (catalina, model SE 200) equipped with a time gated ICCD Camera (1064×1064 pix with 13µm ×13µm pixel size at a binning mode of 1×1 (type Andor , model iStar DH 737-18F). The wavelength scale was calibrated using a low pressure Hg-lamp (Ocean optics). The instrumental bandwidth was measured from the FWHM of the Hg -lines and was found on the average to be 0.12 ± 0.02 nm. Identification of the different lines in the LIBS Spectrum was carried out using Spectrum Analyzer Software version 1.6. The experimental setup including the Optical fiber was absolutely calibrated using a deuterium tungsten halogen lamp (type Ocean optics, model DH 2000 Cal.).

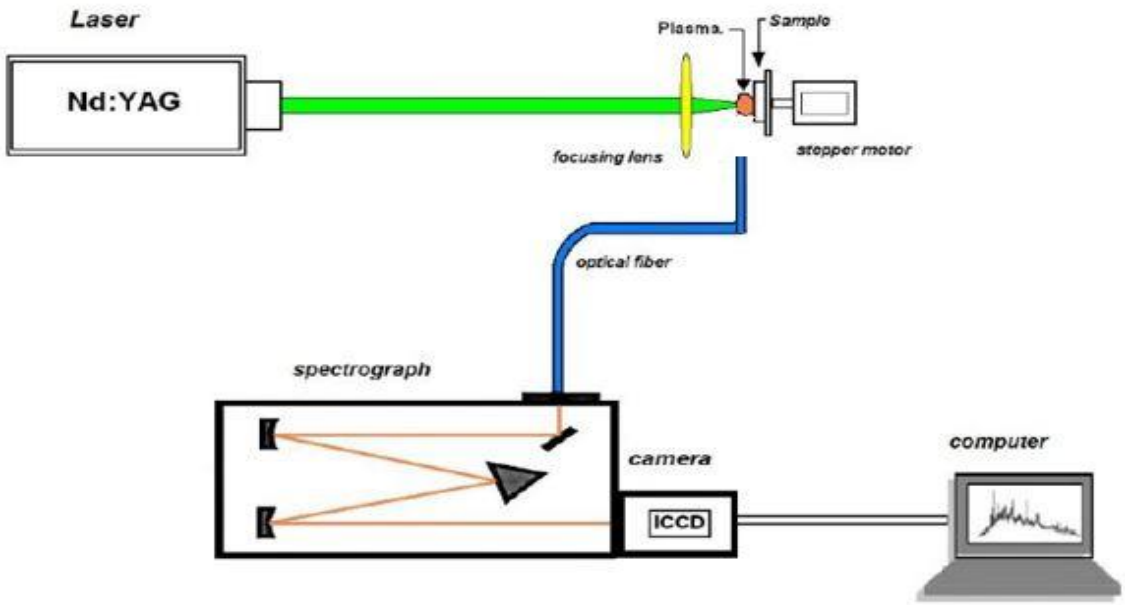

Figure (1): The schematic diagram of the experiment

6. Results and Discussion

6.1. Plasma emission and spectral line analysis:

Figure 2 shows the plasma emission spectra of the aluminum sample. The resonance lines detected were 308.21, 309.27, 394.40, and 396,15 nm have been used to infer the plasma temperature. Assignments of these lines are taken from the NIST data base , and are listed with related details in Table 1. We can observed clearly that the lines spectra are supper imposed on a large continuum component. This continuum is mainly results from the free- free (Bremsstrahlung process) and the free- bound transitions. This continuum should be removed before proceeding in the spectra line shape analysis.

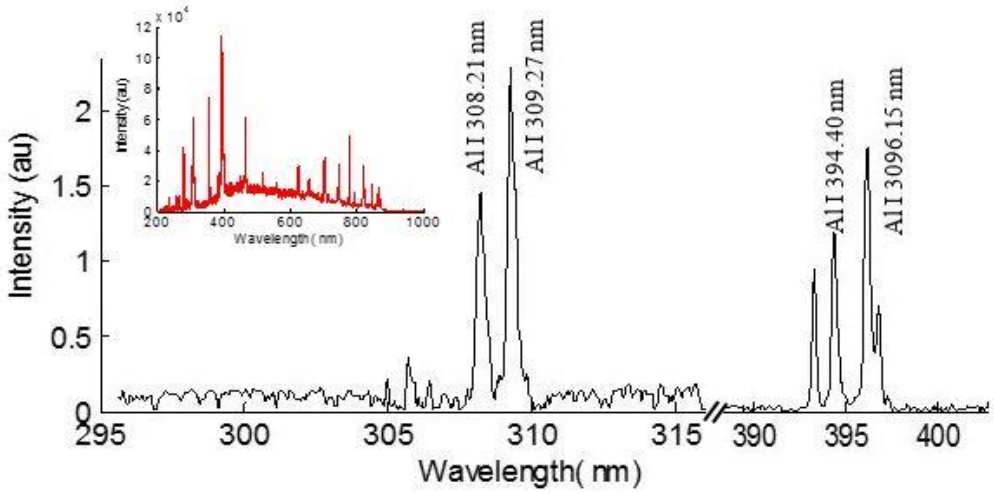

Figure (2): Shows the whole LIBS plasma emission spectra of sample aluminum for wavelength 1064 nm (red color), and the spectral lines lies under study (solid black).

Table 1: Spectroscopic data of aluminum lines.

Element	Wavelength λ(nm)	Transition Probability A(sec^{-1})	Statistical Weight(g)	Excitation Energy (eV)	Transition
Al II	281.61	3.83 $\times 10^8$	1	1.93	$3s^2 3p 4s 1p \rightarrow 3s^2 3p^2 1d$
Al I	308.206	6.30 $\times 10^7$	4	4. 021	$^2D_{3/2}\ p \rightarrow 3p^2\ ^2P_{1/2}$
Al I	309.27	4.93×10^7	5	4. 022	$3d\ ^3D_{3/2} \rightarrow 3p\ ^2P_{3/2}$
Al I	394.40	4.93×10^7	2	3.143	$4s\ ^2S_{1/2} \rightarrow 3p\ ^2P_{1/2}$
Al I	396.15	9.8×10^7	2	3.143	$4s\ ^2S_{1/2} \rightarrow 3p\ ^2P_{3/2}$

6.2. Electron density determination and self-absorption analysis:

In this spectroscopic analysis, the resonance neutral Al lines at 308.21 nm, 309.27 nm, 394.40 nm and 396.15 nm were selected for determining the plasma temperature T_e. The isolated optically thin hydrogen $H_\alpha - line$ at 656.27 nm appeared in the spectrum was used to determine the plasma electron density Ne (Figure 3) and to correct the Al (I) lines which contained some optical thickness. The electron number density in the plume is determined using Eq. (4) for Al(II,I) lines and Eq.(5) for hydrogen line at the wavelength 656.27 nm. It is evident that, in Figures(5-8),the deviation of the measured electron density calculated from the Aluminum neutral lines with respect to that esti-

mated from the optically thin $H_\alpha - line$ indicates the existence of self-absorption while, the aluminum ionic line exhibits a good agreement with $H_\alpha - line$ reminiscent of free from self-absorption as shown in Figure 4.

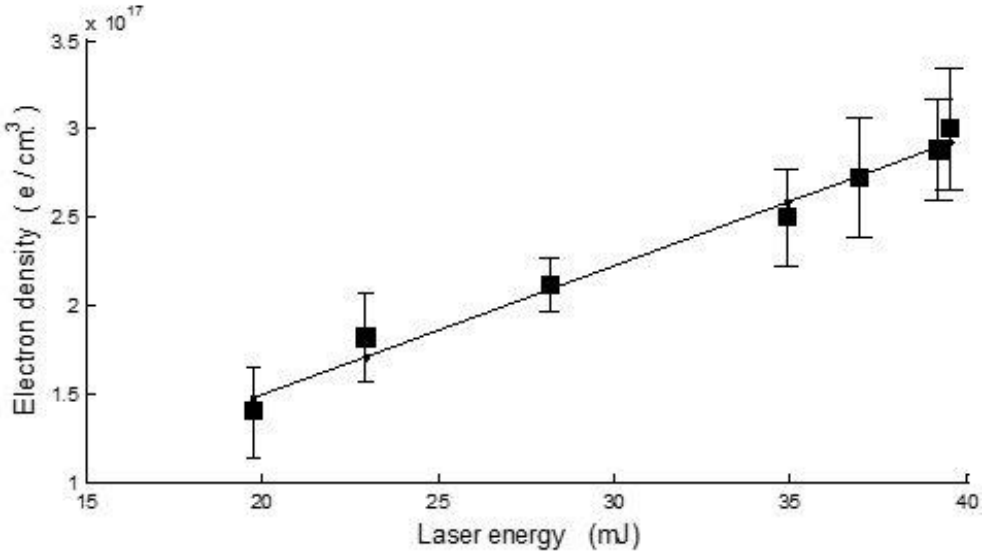

Figure (3): Shows the variation of the electron density of $H_\alpha - line(656.27\ \text{nm})$ with laser energy.

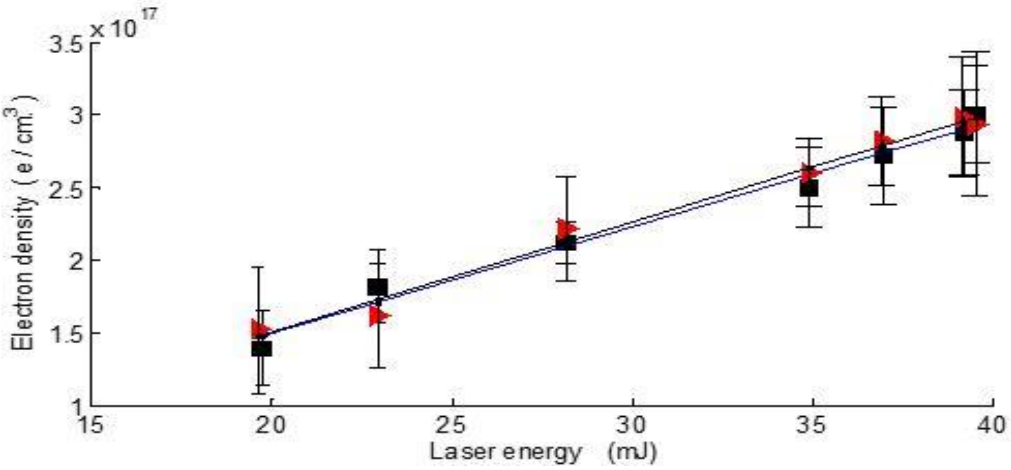

Figure (4): Comparison of electron densities between the $H_\alpha - line(656.27\ \text{nm})$ and Al II (281.61nm) at different laser energies.

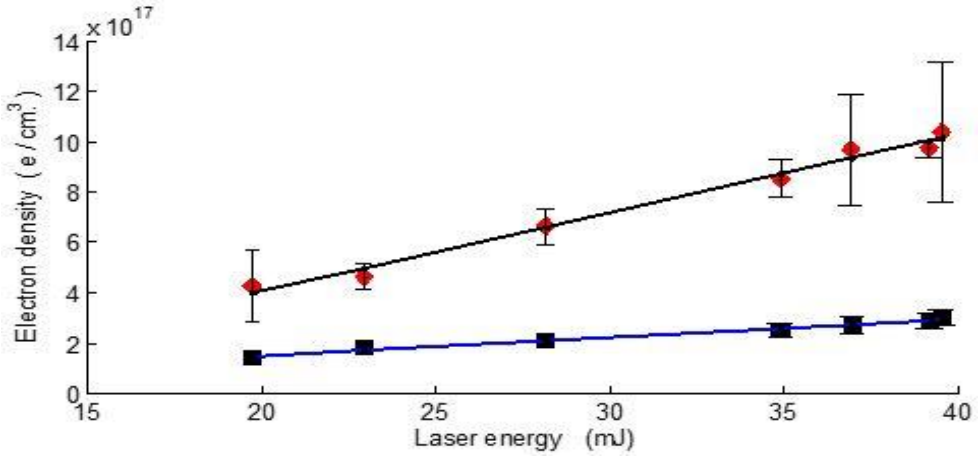

Figure (5): Comparison of electron densities between the $H_\alpha - line$(656.27 nm) and Al I (308.21 nm) at different laser energies.

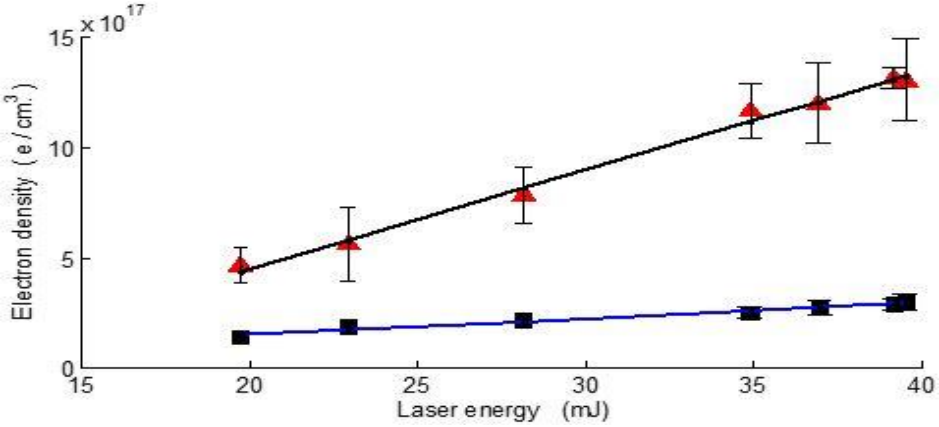

Figure (6): Comparison of electron densities between the $H_\alpha - line$(656.27 nm) and Al I (309.27 nm) at different laser energies.

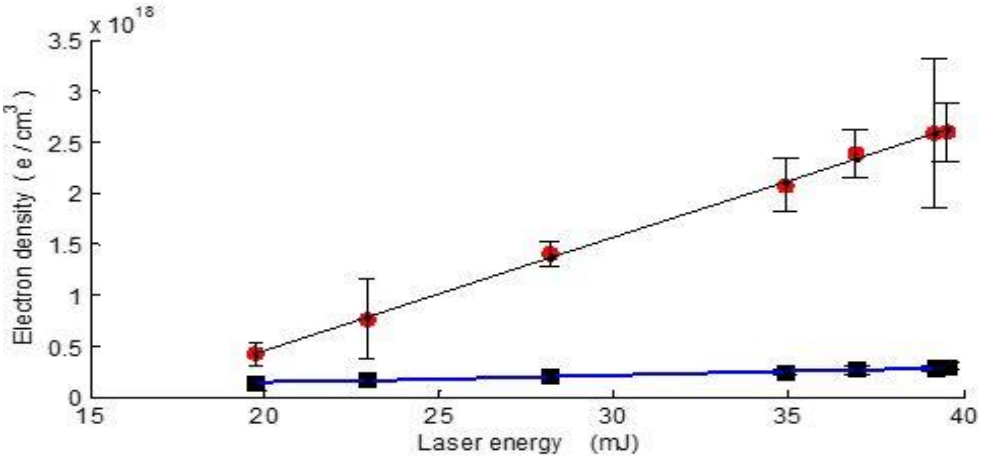

Figure (7): Comparison of electron densities between the $H_\alpha - line$(656.27 nm) and Al I (394.40 nm) at different laser energies.

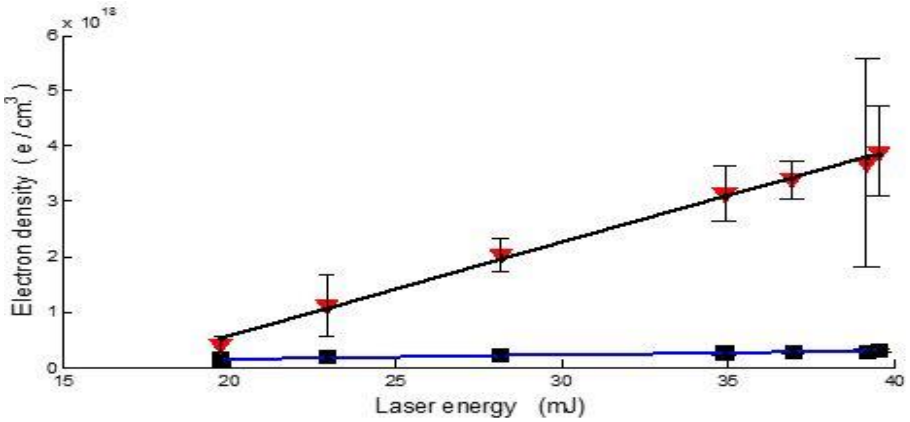

Figure (8): Comparison of electron densities between the $H_\alpha - line(656.27$ nm) and Al I (396.15 nm) at different laser energies.

6.3. Validity of the Local Thermodynamic Equilibrium (LTE):

To determine the electron temperature, the plasma must satisfy the equilibrium conditions, i.e. the plasma must hold a state of local thermodynamic equilibrium during the observation window. In an LTE plasma, the collisional excitation and de-excitation processes must dominate radiative processes and this requires a minimum electron density. The lower limit of the electron density for which the plasma will be verify Eq.(1), where ΔE (eV) is the difference between the upper and lower states and T (eV) is the temperature. For the Al(I) 308.61 nm line transition, $\Delta E = 4.021\ eV$, and the highest electron temperature observed was approximately $1.74eV$. From eq. (1), a minimum electron density of $1.093 \times 10^{16}\ cm^{-3}$ is required for LTE to hold, which is much lower than the $N_e(10^{17} cm^{-3})$ obtained in our experiments. Therefore, local thermodynamic equilibrium is valid for the condition of the present plasma.

6.4. 6. d . Electron temperature determination (Te):

When evaluating the electron temperature using Saha-Boltzmann plot method and the electron number density using spectral line broadening, it is important to correct the intensities of aluminum resonance lines against self-absorption effect according to Eq.(7). On the other hand, Figure 9 shows the Saha-Boltzmann plot for aluminum element. λ and I are the wavelength and the intensity of the spectral lines. The temperature was obtained from the slope of the lines. The plasma temperature of aluminum was 1.44eV before correction against self-absorption effect while became 1.09 eV after the correction, which demonstrates the importance of treatment of self-absorption effect before estimating the plasma temperature .The variation of temperature of Al laser produced plasma in aluminum sample at different laser pulse energies is shown in (Figure 9) below. This figure clearly indicates that with the increase in the laser pulse energy the plasma temperature is also increased. This due to the absorption and /or reflection of the laser photon by the plasma **(Hafeez et al., 2015)**.

ISRAA UNIVERSITY JOURNAL OF APPLIED SCIENCES
ISSN : 2523-0522
Volume 2 : issue 1 , October , 2018

7. CONCLUSION:

A Q-switched laser of Nd: YAG (of 670 mJ per pulse) focused on an aluminum sample, at different laser energies in air, has been used for the plasma diagnosis produced by laser (LPP). The Stark broadening of the H_α – line Hydrogen (656.27 nm) has been used to estimate the electron density of plasma obtained at different laser energies conditions. We have tried measured the electron densities with the profile of the 281.62 nm line of Al II, and the profiles of the 308.21, 309.07, 394.40, and 396,15 nm lines of Al I. The results indicate us that the ionic line doesn't present self-absorption. In contrast the aluminum resonance lines exhibit self-absorption and its usage is inadvisable in plasma temperature estimation. The plasma temperature was calculated before self-absorption quantification and was found to be around 16704 K, while became around 11,000 K after quantification.

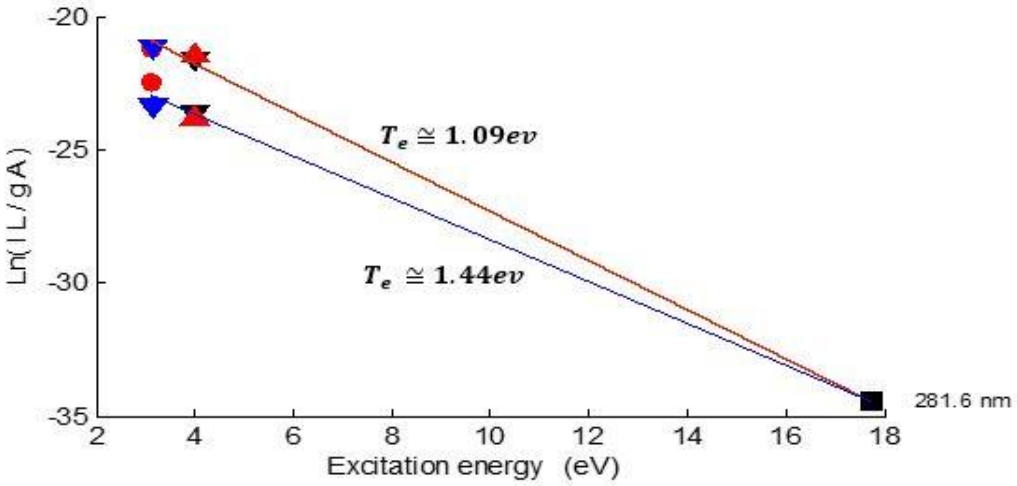

Figure (9): Comparison of Boltzmann plots using Al (I) lines at 308.21 nm, 309.27 nm, 394.40 nm, and 396.15 nm before SA correction and after SA correction

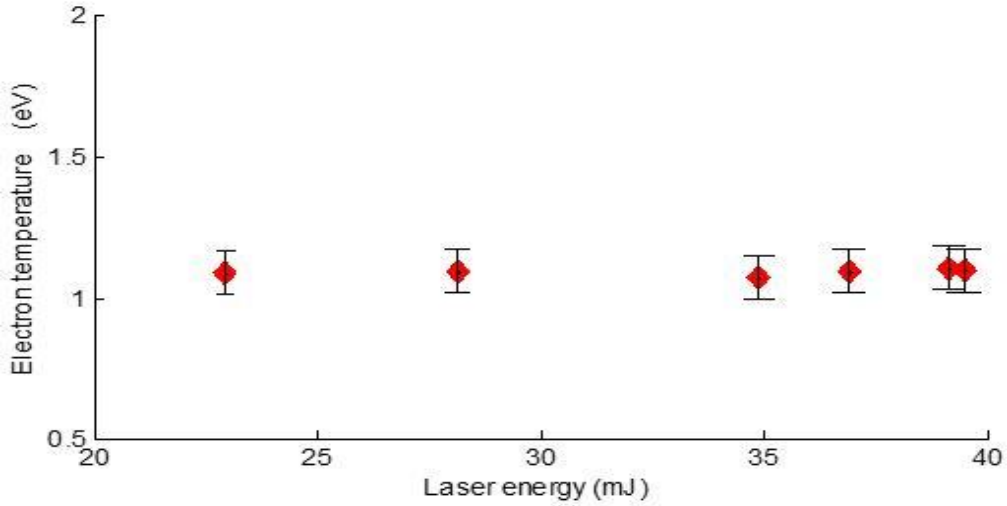

Figure (10): Variation of plasma temperature with laser energy after correction against Self-absorption.

8. ACKNOWLEDGEMENTS

The researcher is thankful to the laboratory of lasers and new materials (LLNM) in Cairo University in Egypt for the encouragement in terms of provision of time and moral support to carry out the research work.

References

5. Almen M.V., (1987) Laser-beam interactions with Materials, Springer-Verlag, New York.
6. Amoruso, S., Armenante, M., Berardi, V., Bruzzese, R. and Spinelli, R., (1997) *Absorption and Saturation Mechanism in Aluminum Laser Ablated Plasmas*. Appl. Physics. A. 65: pp 265-271.
7. Aragón, Bengoechea, A. J., Aguilera, J.A., (2005) *Asymmetric Stark broadening of the Fe I 538.34 nm emission line in a laser induced plasma*, Spectrochim. Acta Part B 60 pp 897–904.
8. Bengoechea, J. J, Aguilera, A., Aragón, C., (2006) *Application of laser-induced plasma spectroscopy to the measurement of Stark broadening parameters*, Spectrochim. Acta Part B 61 pp 69–80.
9. Body, D. and Chadwick, B. L., (2001) *Optimization of the spectral data processing in a LIBS*, Rev. Sci. Instrum., Vol. 72, pp. 1625-1629.
10. Bye, C. A., and Scheeline, A., (2003) *Laser-Induced Breakdown* Spectroscopy *(LIBS) Fundamentals and* Applications. Appli. Spectrosc. 2022-2030.
11. Capitelli, M., Capitelli, F. and Eletskii, A., (2000) *Non-Equilibrium and Equilibrium Problems in Laser-Induced Plasmas*, Spectrochim. Acta Part B. 55: pp 559-574.
12. Colón, C. and Alonso-Medina A., (2006) *Application of a laser produced plasma: experimental Stark widths of single ionized lead lines*, Spectrochim. Acta Part B 61 pp 856–863.
13. Colón, C., Htern, G., Verdugo, P., Ruiz, P., and Campos, J.,(1993) *Measurements of the Stark broadening and shifts parameters for several ultraviolet lines of singly ionized aluminum*, J. Appl. Phys., Vol. 73, no. 10, pp 4752-4758.
14. Cristoforetti, A. g., De Giacomo, A. B., Dell'aglio C. M., Legnaioli, A. E. S., Tognoni, A. V., Palleschi, A. N. and Omenetto, D. (2010) *Local Thermodynamic Equilibrium in Laser-Induced Breakdown Spectroscopy: Beyond The Mcwhirter Criterion*. Spectrochimica Acta Part B. 65: 86-95.
15. Detalle, V., Hóon, M., Sabsabi, M., and St-Onge, I., (2001) *An evaluation of a commercial Echelle spectrometer with intensified charge-coupled device detector for materials analysis by laser-induced laser plasma spectroscopy*, Spectrochim. Acta B, At. Spectrosc., Vol.56, no. 6., pp. 1011-1025.
16. El Sherbini, A., El Sherbini, M. Th, M. Heagzy, H., Cristoforetti, G., Legnaioli, S.,Palleschi, V., Pardini, L., Salvetti, A., Tognoni, E., (2005) *Evaluation of self-absorption of aluminum emission lines in laser-induced breakdown spectroscopy measurements*, Spectrochim. Acta B 60, pp1573–1579.
17. Fujimoto, T., (2004) Plasma Spectroscopy. Clarendon Press, Oxford.
18. Griem H.R., (1964) Spectral Line Broadening by Plasmas, Academic Press, New York.
19. Griem, H.R., (1974) Spectral Line Broadening by Plasmas. Academic Press, New York.
20. Hafeez, S., Shaikh, N. M. and Baig M. A., (2008) *Spectroscopic studies of Ca plasma generated by the fundamental, second, and third harmonics of a Nd:YAG laser*, Laser and Particle Beams 26 pp41.

21. Handoko, A. D., Lee, P. S., Lee, P., Mohanty S. R., and Rawat, R. S., (2006) *Time resolved emission spectroscopy*, J. Phys.: Conf. Ser., Vol. 28, pp 100-104.

22. Kepple P., and Griem H.R., (1968) *Improved Stark Profile Calculations for Hydrogen Lines: H_α, H_β,H_δ and H_γ*, Physical review, 173 pp 317-325.

23. Kim, D. E., Yoo, K. J, Park, H. K., Oh, k. J., and Kim, D. W., (1997) *Quantitative analysis of aluminum impurities in Zinc alloy*, Appl. Spectrosc., Vol. 51, no.1, pp 22-29.
24. Konjevic N., (2003) *Plasma Broadening and Shifting of Non-Hydrogenic Spectral Lines: Present Status and Applications*, Physics Reports, 316 pp 339- 401.
25. Konjevic N., Lesage A., Fuhr J. R. and Wiese W. L., (2000) *Experimental Stark Width for Spectral Lines of Neutral and Ionized Atoms (A Critical Review of Selected Data For the Period 1989 through2000*,Journal of Physical and Chemical Reference Data, 31 pp 819- 927.
26. Le Drogoff, B., Margot, J., Chacker, M., Sabsabi, M., Barthelemy, O., Johnston, T. W., Laville, S., Vidal, F., and von Kaenel, y., (2001) *Temporal characterization of femtosecond laser*, Spectrochim. Acta B , At. Spectrosc., Vol. 6, no. 6, pp 987-1002.
27. Lee, Y. L., Sawan, S. P., Thiem, T. L., Teng, Y.-Y., and Sneddon, j., (1992) *Interaction of a laser beam with metals, part II: Space-resolved studies of laser-ablated plasma emission*, Appl. Spectrosc., Vol. 46, no.3, pp. 436-441.
28. Lu, Y., Tao, z., and Hong, M., (1999) *Characteristics of excimer laser induced plasma from an aluminum target*, Jpn. J. Appl. Phys., Vol.38, no. 5A, pp 2958-2963.
29. Mansour S. A., (2015) *Self-Absorption Effects on Electron Temperature Measurements Utilizing Laser Induced Breakdown Spectroscopy (LIBS)-Techniques*, Optics and Photonics Journal, 5 pp79-90.
30. Mansour S. A., El Sherbini A. M., Allam S. H., El Sherbini Th. M., (2015) *Optical Spectroscopic Studies of Silicon Plasma Produced by Fundamental (1064) of an Nd: YAG Laser*, Australian Journal of Modern Physics,2 pp1-13.
31. Mansour S. A., El Sherbini A. M., Allam S. H., El Sherbini Th. M., (2017) *Spectral Studies of Nanosecond Laser Interaction with Aluminum-Based Alloy Containing Traces of Magnesium in Air*, Israa University Journal of Applied Science,1 pp55-67.
32. McWhirter R. W. P, (1965) Plasma Diagnostic Techniques Pure and Applied Physics vol. 21eds Huddlestone R H and Leonard S. L. (New York: Academic Press) 201-264.
33. Miziolek, A. W., Palleschi, V. and Schechter, I., (2006) *Laser-Induced Breakdown Spectroscopy (LIBS) Fundamentals and Applications*. Cambridge University Press, United Kingdom, Britain.
34. NIST Atomic Spectra Database (ver. 5.4), http://physics.nist.gov/asd (2017).
35. Sabsabi, M., and Cielo, P., (1995) *Quantitative analysis of aluminum alloys by laser-induced breakdown spectroscopy* , Appl. Spectrosc., Vol. 49, no. 4, pp. 499-507.Yalcin S., Crosley D. R., Smith G. P. and Faris G.W.(1999) *Influence of Ambient Conditions on The Laser Air Spark*, Applied Physics: B Laser and Optics, 68 pp 121-130.
36. Thoron, A. P., (1988) Spectroscopic, 2nd ed. London, U.K.: Chapman & Hall.
37. Tognoni, E. Palleschi, V. Corsi, M. Cristoforetti, G., (2002) *Quantitative microanalysis by laser-induced breakdown spectroscopy: a review of the experimental approaches*, Spectrochim. Acta Part B 57 pp1115–130.
38. Van Der Mullen, J. M. N., (1990) *On the Atomic State Distribution Function in Inductively Coupled Plasmas -The Stage of Local Thermal Equilibrium and its Validity Region*. Spectrochim Acta Part B. 45: 1-13.